Supporting Information

Motility-dependent selective transport of active matter in trap arrays: Separation methods based on trapping-detrapping and deterministic lateral displacement

Vyacheslav R. Misko[a,b,*], Franco Nori[b,c,d] and Wim De Malsche[a]

a) *µFlow group, Department of Chemical Engineering, Vrije Universiteit Brussel, Pleinlaan 2, 1050 Brussels, Belgium*
b) *Theoretical Quantum Physics Laboratory, Cluster for Pioneering Research, RIKEN, Wako-shi, Saitama 351-0198, Japan*
c) *Quantum Computing Center, RIKEN, Wako-shi, Saitama, 351-0198, Japan*
d) *Physics Department, University of Michigan, Ann Arbor, Michigan 48109-1040, USA*

1. Trapping-detrapping mechanism of motile particle separation in arrays of traps

The trapping-detrapping mechanism of motile particle separation in arrays of traps is a rather robust mechanism. Indeed, it requires the following relation between the maximum trapping force due to the trap, that keeps a particle inside the trap, and the Stokes drag force due to the fluid flow, that facilitates the escape of the particle from the trap. For a passive particle, the trapping force should be larger than the drag force to keep it inside the trap. Under the same condition, motile particles can escape the trap due to their additional self-propulsion velocity (that in the overdamped limit is proportional to the force).

In Figs. S1 and S2, this separation mechanism is illustrated for various set of parameters.

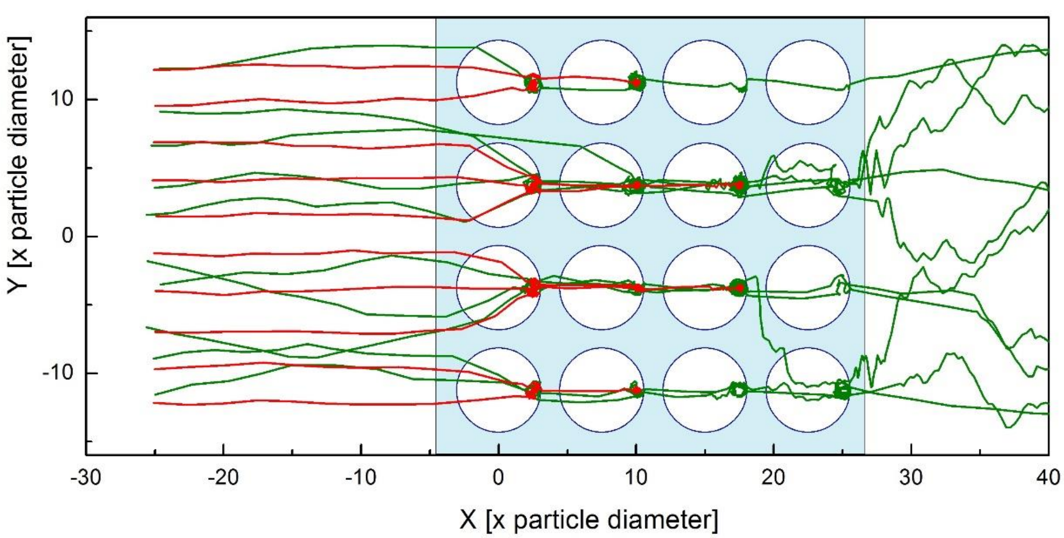

Fig. S1. Selective trapping of particles depending on their motility in an array of traps of radius R = 3.2. The array period is 7.5, and the gap (in the x- and y-direction) between the traps is 1.1. The trajectories of passive particles are shown by red colour, and the trajectories of active particles (Janus particles or motile cells) characterized by self-velocity, v_0, are shown by green colour. A mixture of passive and active particles is infused from the left side. It is driven by a transport flow with velocity v_{flow}, which is chosen as the unit of velocity. The self-propelled velocity is $v_0 = 0.25v_{flow}$. The maximum trap strength, F_p = 2.5 ("deep" traps). Both species, active and passive, are trapped, and active particles escape the traps and, through a series of trapping-detrapping events, reach the right-side chamber of the device and are collected separately. Passive particles remain trapped.

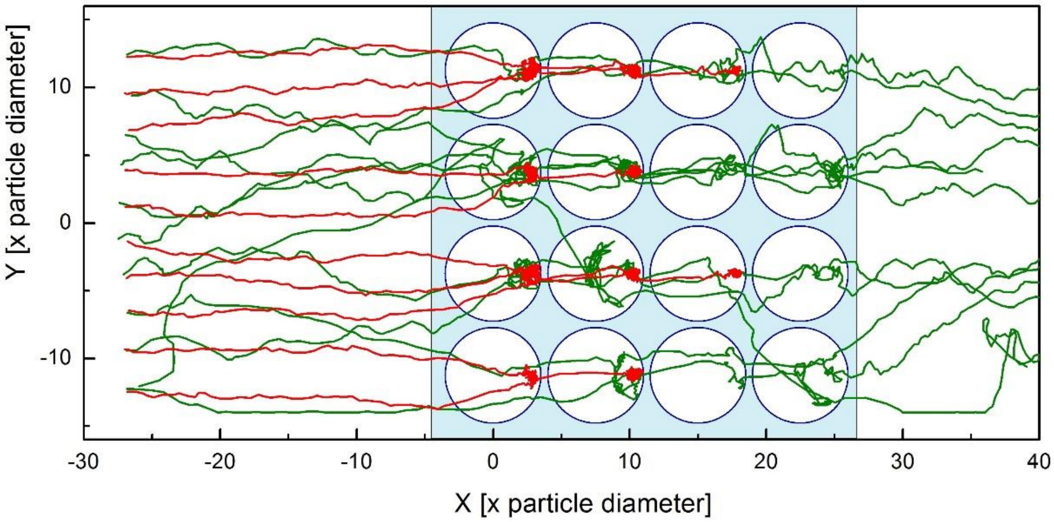

Fig. S2. Same as in Fig. 1, but for traps of radius R = 3.5. The gap between the traps is 0.5. The self-propelled velocity is $v_0 = 0.625 v_{\text{flow}}$. The maximum trap strength, F_p = 0.5 ("shallow" traps).

2. Motile particle separation in DLD-type arrays of traps

Separation of motile particles in a DLD-type array of traps requires a gentle balance between the key parameters of the method, i.e., the angle of the infused flow with respect to the DLD array axis as well as the flow rate and the self-propelled velocity. In this section, we demonstrate the effect of the radius of the trap, the self-propulsion velocity, and the persistence time (length) on the separation efficiency of motile particles from immotile species.

First, the effect of the trap radius on the guiding efficiency of passive particles is demonstrated in Fig. S3. The ability of a DLD array of traps of guiding passive particles (i.e., the "displacement mode") is crucial for an efficient separation. It can be considered as a "calibration" condition of a DLD array (also in potential experiments). Indeed, we should first find a set of parameters when passive particles follow the "displacement mode", at a large enough angle between the direction of the flow and that of the DLD array. As illustrated in Fig. 3S, increasing diameter of the traps facilitates the realization of the "displacement mode" for passive particles.

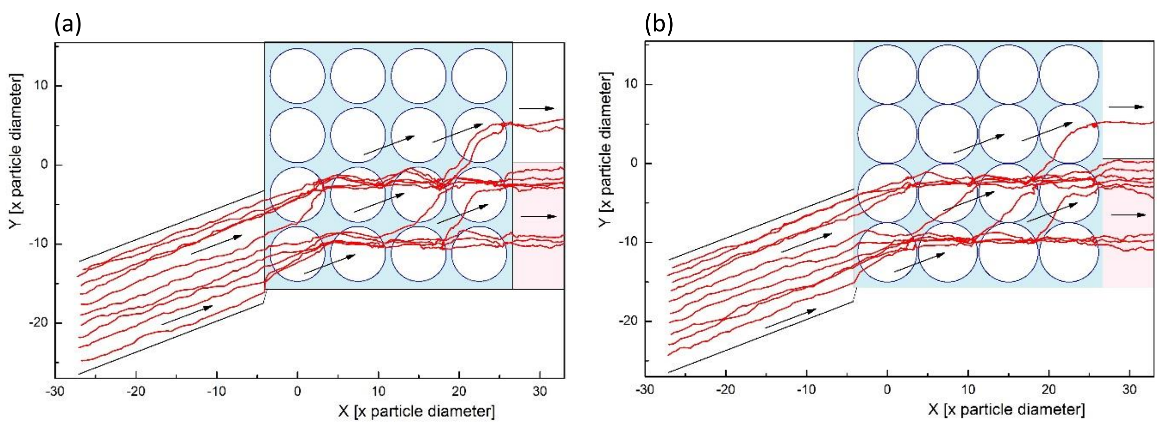

(c)

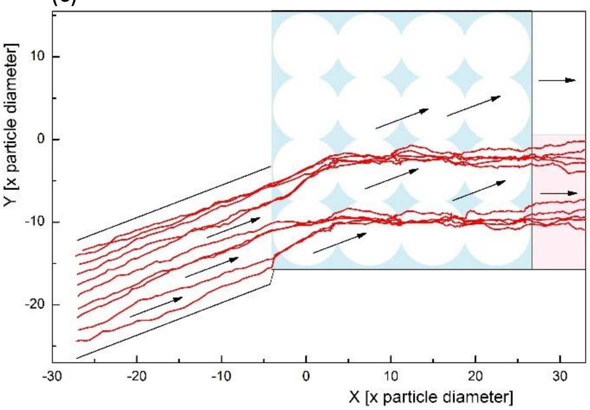

Fig. S3. The effect of guiding passive particles along the direction of rows of traps in a DLD separation device, for varying radius of the traps: R = 3.5 (a), 3.75 (b), and 4.0 (c). The corresponding efficiency of the guiding is: 0.8 (a), 0.9 (b), and 1.0 (c). The angle between the direction of the flow and the array row (infusion angle) is γ = 21.8°.

Large traps are more efficient in guiding passive particles. The most efficient geometry is an array of overlapping traps. This geometry can be experimentally realized, e.g., by using microwell arrays (described in Sec. 5 of the main text).

Once the condition for the realization of the "displacement mode" for passive particles is found, active particles can be added to the consideration. Figure S4 illustrated the effect of the self-propulsion velocity on the efficiency of separation of motile particles from passive beads.

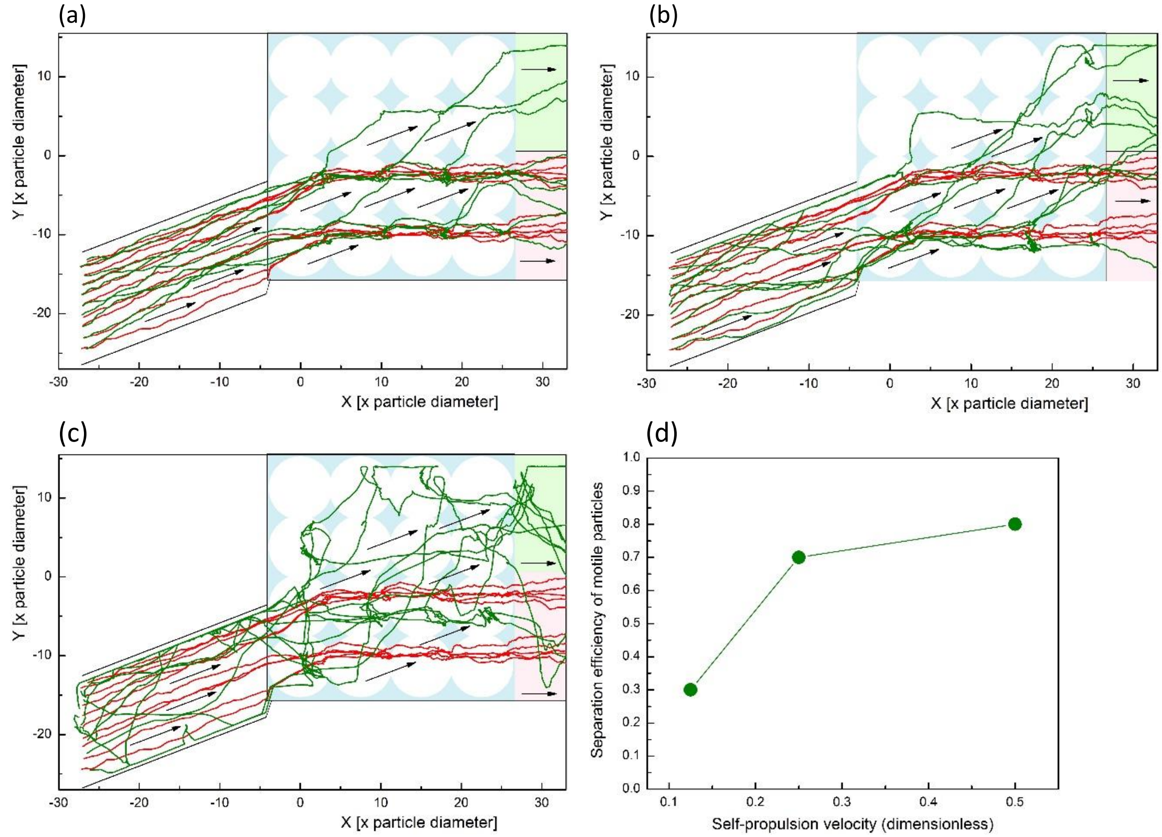

Fig. S4. The impact of the self-propulsion velocity on the efficiency of separation of motile particles from immotile particles in a DLD-type trap array with a radius of a trap, R = 4.0, for varying self-propulsion velocity, v_0 = 0.125 (a), 0.25 (b), and 0.5 (c). The corresponding efficiency of separation as a function of v_0 is presented in (d). The flow velocity is, v_{flow} = 0.45, and the rotational diffusion coefficient, D_r = 0.01. The angle between the direction of the flow and the array row (infusion angle) is γ = 21.8°. The black arrows show the direction of the flow.

As it follows from Fig. S4, the efficiency of separation of motile particles from passive particles increases with increasing self-propulsion velocity. Indeed, the value of self-propulsion velocity is a parameter that distinguishes motile particles from immotile (v_0 = 0 for immotile particles), and therefore the separation efficiency increases with increasing self-propulsion velocity. However, a very high self-propulsion velocity can result in re-entrance of passive particles in the flow of passive particles. Therefore, the flow velocity should be adjusted to avoid this re-entrance that could suppress the separation efficiency.

Next, let us analyse the impact of the rotational diffusion coefficient, D_r (or the persistence time, $\tau = 1/D_r$) on the efficiency of separation. Rotational diffusion is another key parameter of self-propelled motion that distinguishes it from thermal Brownian motion of passive beads. The corresponding results are presented in Fig. S5.

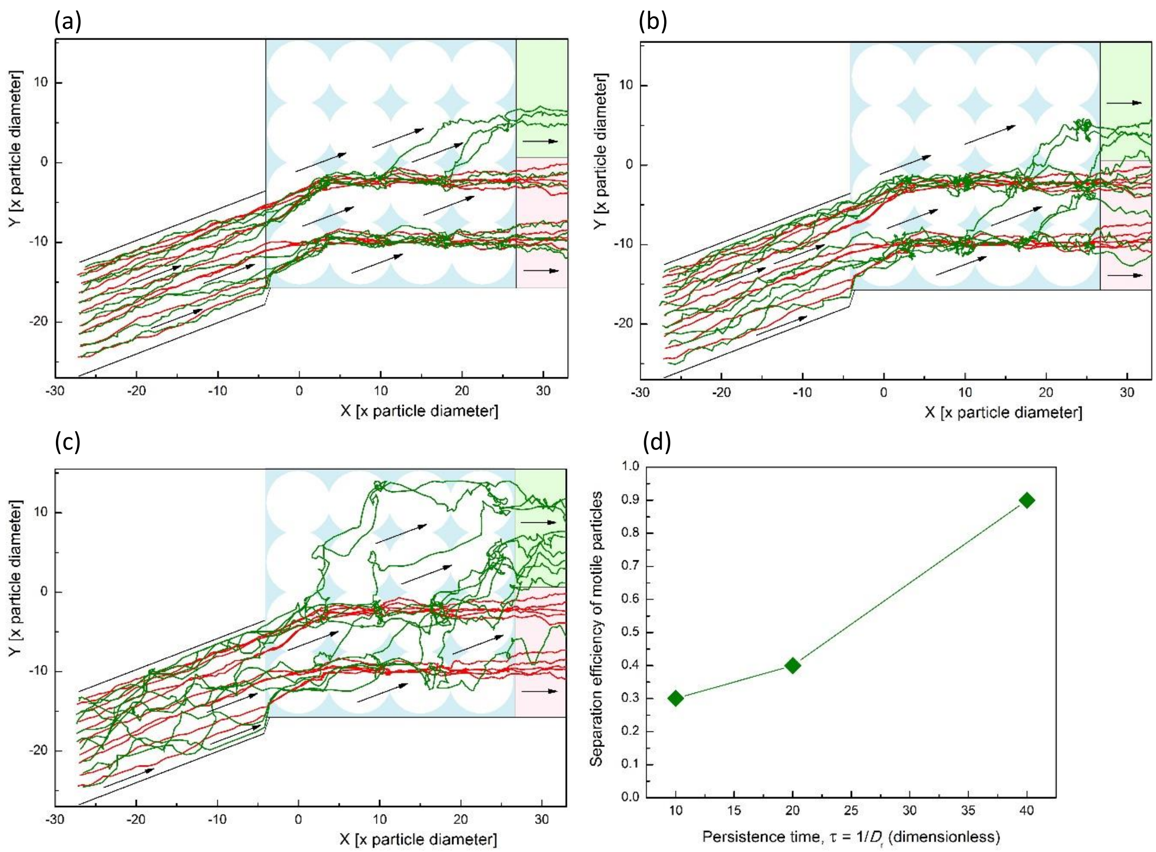

Fig. S5. The impact of rotational diffusion on the efficiency of separation of motile particles from immotile particles in a DLD-type trap array with a radius of a trap, R = 4.0, for varying rotational diffusion coefficient, D_r = 0.1 (a), 0.05 (b), and 0.025 (c). The corresponding efficiency of separation as a function of $\tau = 1/D_r$ is presented in (d). The flow velocity is, v_{flow} = 0.45, and the self-propulsion velocity, v_0 = 0.5. The angle between the direction of the flow and the array row (infusion angle) is γ = 21.8°. The black arrows show the direction of the flow.

As shown in Fig. S5, the separation efficiency is very low for large rotational diffusion even despite the high value of self-propulsion velocity. This result can be understood as follows. Strong rotational diffusion means that a particle rapidly reorients, and its motion becomes similar to thermal Brownian motion. This striking effect was previously discussed in the context of rectification of self-propelled motion, in Ref. [6] (see the main text). A particle executes fast movements, but these are chaotic. This situation resembles the Brownian motion at a high temperature. It is clear therefore that in this case the separation efficiency is low. This behaviour also resembles the motion of motile sperm cells characterized by high velocity but very short persistence length. In terms of motility grades, such sperm cells are referred to grade C (see Ref. [35] in the main text) and are considered not suitable for artificial fertilization as these are not capable of executing a propulsion in a straight direction.

It is interesting to analyse, whether the effect of strong rotational diffusion discussed above can be compensated by increasing self-propulsion velocity. For this purpose, we consider motile particles characterized by the rotational diffusion coefficient, D_r = 0.1 (the least favourable for separation case presented in Fig. S5), and high values of the self-propulsion velocity, v_0 = 1.0 and v_0 = 2.0. This situation is presented in Fig. S6.

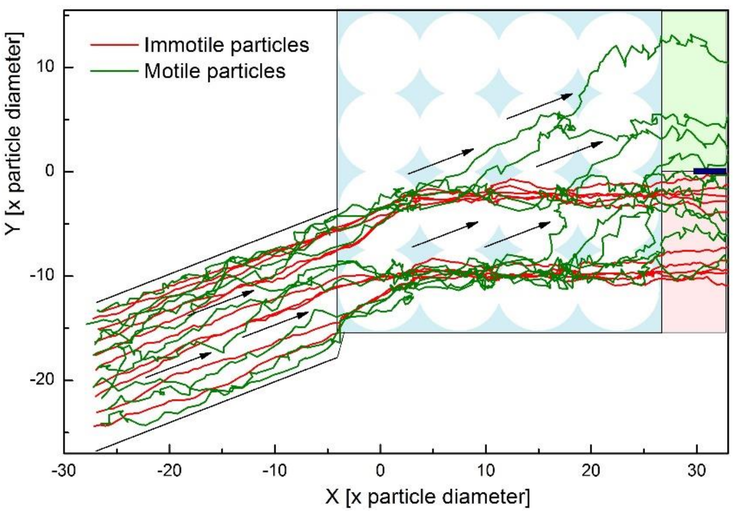

(a)

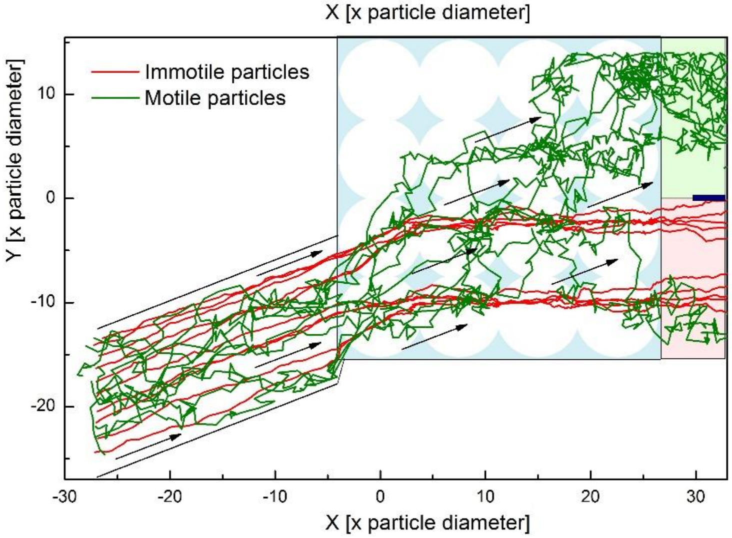

(b)

Fig. S6. The impact of the self-propulsion velocity on the efficiency of separation of motile particles from immotile particles in a DLD-type trap array with a radius of a trap, R = 4.0, for high self-propulsion velocity, v_0 = 1.0 (a), 2.0 (b). Here, v_{flow} = 0.45, D_r = 0.1. The angle between the direction of the flow and the array row (infusion angle) is γ = 21.8°.

The results of the analysis presented in Fig. S6 demonstrate therefore that the effect of strong rotational diffusion (resulted in a suppression of the efficiency of separation) can be compensated by increasing self-propulsion velocity. While for D_r = 0.1 and the self-propulsion velocity v_0 = 0.5 (shown in Fig. S5(a)) the separation efficiency is only 0.3, and it is 0.4 for v_0 = 1.0 (Fig. S6(a)), the separation efficiency reaches the value of 0.9 for v_0 = 2.0 (Fig. S6(b)).

Finally, let us consider the effect of focusing of the infusion flow that carries the mixture of motile and immotile particles. For this purpose, we reduce the width of the inlet channel by a factor of 0.5, as shown in Fig. S7 and study the separation efficiency for varying self-propulsion velocity. Also, we reduce the diameter of the traps such that these do not overlap (cp. Figs. S4, S5, and S6). This geometry of the trap array is easier to realize, and it can be also realized with separate vortices.

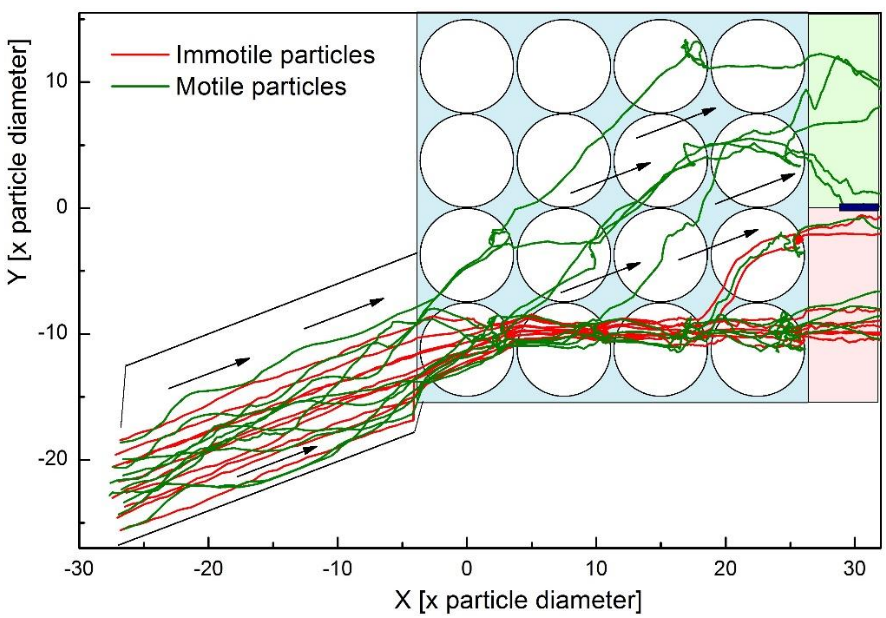

(a)

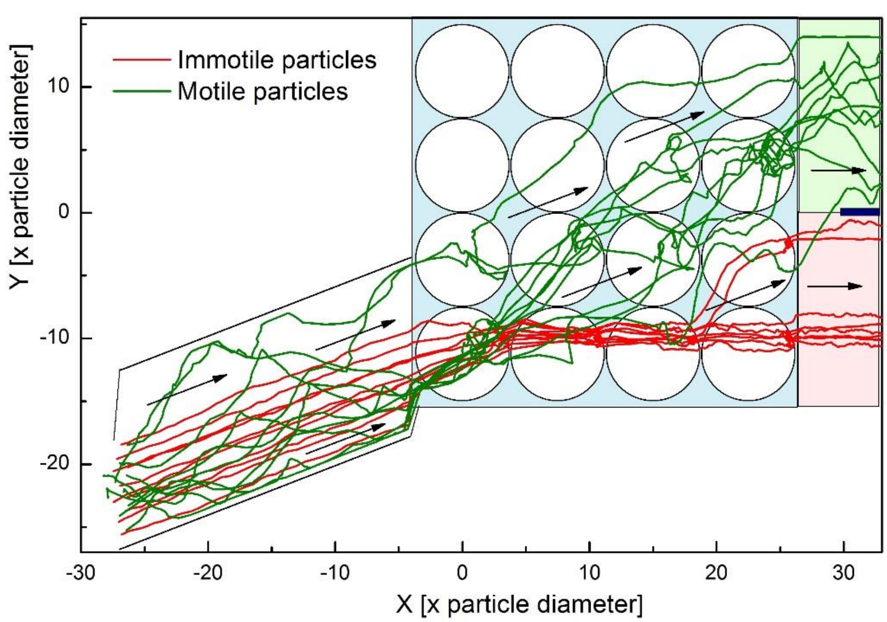

(b)

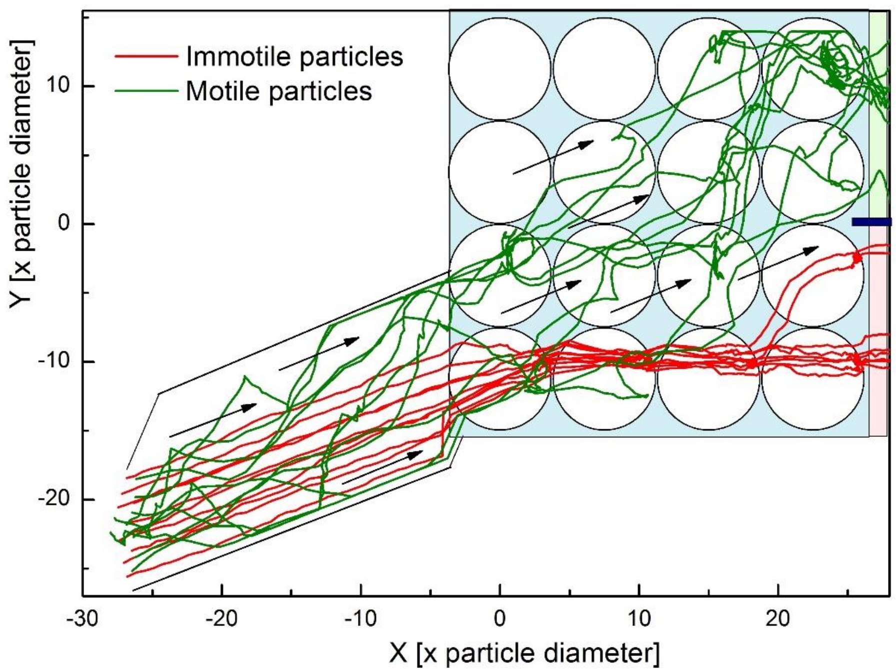

(c)

Fig. S7. The impact of the self-propulsion velocity on the efficiency of separation of motile particles from immotile particles in a DLD-type trap array with a radius of a trap, R = 3.75, for self-propulsion velocity, v_0 = 0.25 (a), 0.445 (b), and 0.55 (c). Here, v_{flow} = 0.57, D_r = 0.024. The angle between the direction of the flow and the array row (infusion angle) is γ = 21.8°. The width of the inlet channel for infusion of particles is reduced by a factor of 0.5.

Therefore, the results shown in Fig. S7 demonstrate that the additional modification of the setup, i.e., the reduction of the width of the inlet channel, allowed us to enhance the efficiency of separation up to the maximum value, 1.0, even for moderate values of the self-propulsion velocity.

The above analysis shows that separation of motile from immotile particles (motile cells from immotile cells), using the proposed separation techniques, can be achieved for broad range of parameters. This analysis reveals the relations between the parameters that result in efficient separation. It also provides guidelines for potential experimental realizations of the predicted separation methods using arrays of traps. The conversion of the dimensionless units used in the simulations, to the dimensional units is straightforward, as we provide the relations between the values. For example, if the unit of length is 1 μm, and the unit of time is 1 s, then velocities are measured in μm/s (and the force exerted on a particle due to the flow can be found from the Stokes formula, Eq. (6) of the main text), and the corresponding diffusion coefficients can be either calculated theoretically or extracted from the experimental measurements of the mean-squared displacement (MSD) as discussed in the main text (Sec. 6, "Methods"). However, for self-propelled particles it would be more reliable to calculate the diffusion coefficients from experimental measurements of the MSD as Janus particles can acquire an additional torque due to, e.g., an asymmetry of the cover layer.